

RAW MATERIAL SOURCES FOR THE ROMAN BRACARENSE CERAMICS (NW IBERIAN PENINSULA)

M. ISABEL PRUDÊNCIO¹, M. AMÁLIA SEQUEIRA BRAGA², FELISBELA OLIVEIRA³, M. ISABEL DIAS^{1,*},
MANUELA DELGADO⁴ AND MANUELA MARTINS⁴

¹ Instituto Tecnológico e Nuclear, EN 10, 2686-953 Sacavém, Portugal

² Centro de Investigação Geológica, Ordenamento e Valorização de Recursos (CIG-R), Universidade do Minho, Campus de Gualtar, 4710-057 Braga, Portugal

³ Gabinete de Arqueologia, Câmara Municipal, 4760-110 V. N. Famalicão, Portugal

⁴ Unidade de Arqueologia, Universidade do Minho, 4700-320 Braga, Portugal

Abstract—The Bracarense ceramics are characterized by a fine, pale yellow paste covered with a brownish yellow slip. The name is derived from Bracara Augusta, the Roman town located in the north of Portugal, where this type of ceramic paste was first found and identified. Various forms with the same type of paste occur, such as imitations of sigillata, terra sigillata and thin walls from the Augustus-Tiberius period, and common ware. Later, similar ceramics were also found in other archeological sites, *e.g.* Aquis Querquennis (Galiza, Spain), which question the location of the production center of this type of ceramic paste.

Mineralogical and chemical analyses showed that the majority of the Bracarense shards studied differ from the common ware of the Braga region. Despite minor differences, the Bracarense shards collected in Aquis Querquennis have the same geochemical pattern as those found in Bracara Augusta, *i.e.* they appear to have been manufactured with the same clay type. The firing products found indicate a kaolin character of the source clay, and point to firing temperatures near 900°C. The Aquis Querquennis shards have greater Br contents, which can be explained by use-wear and/or post-depositional processes, as this site is located in a thermal-water region.

Key Words—Archeological Ceramics, Clays, INAA, Mineral Transformation, Mullite, Production Technology, SEM-EDS, Spinel, Trace Elements, XRD.

INTRODUCTION

Bracara Augusta, Braga (NW Portugal), was a Roman town recognized as a center of production and distribution of pottery to a wide regional area (Martins and Delgado, 1995). The morphological analysis of Roman ceramics established the existence and chronology of different production types used during the long Roman occupation of the town (five centuries). From the study of thousands of shards found in Braga, different types of Roman pottery were recognized, such as Bracarense, polished fine gray painted ceramics, late gray ceramics, local amphorae production, non-vitreous red slips ware and several types of common ware (Martins and Delgado, 1989–90a, 1989–90b). The existence of production centers in Bracara Augusta and vicinity has been demonstrated using the so-called criterion of abundance or gravity model (Rice, 1987), as there is no clear archeological evidence of pottery workshops in the Braga region. Chemical and mineralogical characterization of the pastes of different types of ceramics found in Bracara Augusta has been carried out in an

attempt to confirm the morphological classification by macroscopic observation of the pastes (Oliveira, 1997; Gomes, 2000; Gaspar, 2000; Oliveira *et al.*, 2005). While provenance studies may be able to identify the kinds of clay material used in a particular kind of pottery, they do not provide information on the cultural or socioeconomic context, such as the locations of workshops, which depends on the finding of kilns, deposits of raw materials, wasters, *etc.* at a site. The approach adopted for the establishment of the existence of ceramic production in Bracara Augusta (town and its vicinities) has been a combination of the abundance of the types of potteries (forms and paste types) and comparisons of the ceramic composition with resources available in the area.

The inventories of the regional clay materials and their mineralogical characterization were reported previously (Sequeira Braga, 1988; Ferreira *et al.*, 2000). These materials occur in the Cávado river basin, NW Portugal, between the city of Braga and the shoreline. According to these authors, during the Tertiary, tropical climatic conditions led to ferrallitic weathering, which can be observed in Espinheira-Quebrosas and Ucha. This relic of paleoweathering is characterized by a massive kaolinitic mantle with goethite concretions, which were preserved by horst and graben tectonics of the Pliocene. Local reworking and the transport and deposition of

* E-mail address of corresponding author:

isadias@itn.mcies.pt

DOI: 10.1346/CCMN.2006.0540510

those paleoweathering deposits in temporary basins produced deposits of siderolitic facies with kaolinite, goethite and hematite outcrops in Espinheira and Quebrasas. Arenaceous terraces younger than Pliocene built of fluvial and lacustrine deposits are associated with arenization processes along the Cávado river basin. A synthesis of the granitic saprolites and arenization in NW Portugal was previously published by Sequeira Braga *et al.* (2002). The principal features of granite weathering in a temperate climate are: saprolite depths of >10 m; mean material loss of 40 wt.%; small clay content (mean value of 7 wt.%); and a high degree of mineralogical evolution. The clay fraction is characterized by a predominance of kaolinite and gibbsite with subordinate 2:1 minerals (illite, chlorite, vermiculitic mixed layers and vermiculite). These previous geological studies, including the inventories of regional clay materials and their mineralogical characterization have been used in tracing the clays in the aforementioned archeometric studies.

Among the several types of ceramics found in Bracara Augusta, special attention is paid in this work to the Bracaraense, a fine Roman ceramic with a pale yellow paste covered with a brownish yellow slip (Alarcão and Martins, 1976; Oliveira, 1997) that is clearly different from other ceramic types found in the town. The same fine yellowish paste is found in some common wares and special ceramic pieces, such as imitations of sigillata, terra sigillata, and in thin walls from the Augustus Tiberius period. Common wares, as well as imitations of imported wares, such as terra sigillata and Pompeian slip, were also probably produced locally, using raw materials available close to the Roman town (Oliveira, 1997; Gomes, 2000; Gaspar, 2000; Oliveira *et al.*, 2005).

The name – Bracaraense – was chosen because it was first located and identified in the Bracara Augusta area. Later on, similar pottery shards were found in other archeological sites of the NW Iberian Peninsula region, such as Aquis Querquennis (Galiza, Spain), which, together with the absence of kilns near Braga, lead to questions about the location of the production center.

Aquis Querquennis, Bande (Ourense region, Galicia, NW Spain), is located at the *vía XVIII* of the Antonino itinerary, which connected Bracara to Asturica (Astorga, Spain). Aquis Querquennis is a large archeological complex, including several structures, namely the military camp, a possible inn facing the *XVIII vía*, one thermal-waters bath complex, local pre-Roman settlements and Roman villas (Rodríguez Colmenero, 1983; Hervés Raigoso, 1989). This site and surrounding area are characterized by granite. One outcrop of these granites located in the Celanova-Bande area consists of heterogeneous granitoids exhibiting diverse structures of migmatitic type (ITGE, 1989).

The chief goals of this study were to discover if the Bracaraense ceramics from the two sites are similar in

composition, and to identify the geographical source region by tracing the clay source used. The procurement of clays to study in this work was directed to the more suitable raw materials, taking into account the fine grain size and color characteristics of the Bracaraense ceramic paste. The objectives were achieved by a mineralogical and geochemical study of the ceramic paste and the clay materials available in the area. Due to the fine grain size and small thickness of the walls of the shards, optical and scanning electron microscopy (SEM) were performed only for selected samples.

EXPERIMENTAL

Pottery shards from Bracara Augusta (27 samples) and Aquis Querquennis (eight samples) as well as whole samples of clay materials (20 samples) were prepared for mineralogical and chemical analyses. The localities sampled are shown in Figure 1. Among the numerous clay materials available in the region and those still exploited at the present day, a selection of the possible source materials was carried out. Clay materials derived by weathering of granites and schists as well as sedimentary deposits, located between the city of Braga and the shoreline (Figure 1), were sampled at: (a) Campados – residual kaolin deposit derived by weathering of Campados granite (#1); (b) Barqueiros – sedimentary kaolin deposit (#2); (c) Espinheira and Bustelo – clays derived by weathering of schists (#3 and 4); (d) Ucha and Quebrasas – sedimentary deposits located near Braga (#5 and 6); and (e) Braga – residual clay materials derived by weathering of the Braga granite (#7).

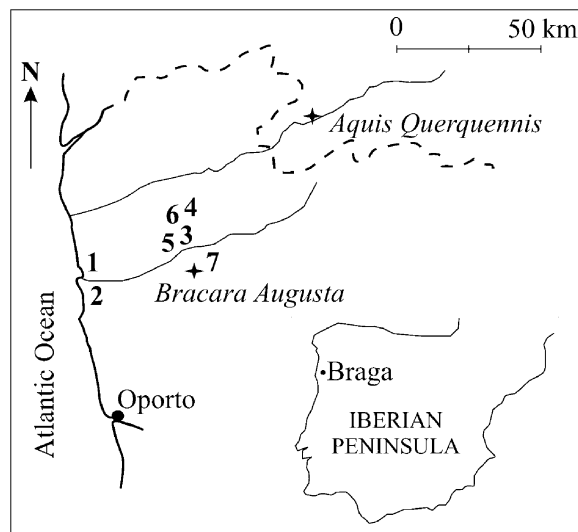


Figure 1. Map of the studied area, with the locations of the archeological sites (✚) Bracara Augusta and Aquis Querquennis, and the areas where the clay materials were sampled. 1 – Campados; 2 – Barqueiros; 3 – Espinheira; 4 – Bustelo; 5 – Ucha; 6 – Quebrasas; 7 – Braga.

The shards were examined by optical microscopy, X-ray diffraction (XRD), and SEM with an energy dispersive spectrometer (EDS) for chemical analysis. Standard ZAF corrections allowed semi-quantitative microanalyses for characterization of mineralogical phases. The whole sample of the pastes, and the source clay samples, were also analyzed by XRD and instrumental neutron activation analysis (INAA).

Two separate pieces $\sim 2 \text{ cm}^2$ in area were removed from the shards ($\sim 2 \text{ g}$ potsherd) for mineralogical and chemical analyses of the ceramic paste (whole sample) by XRD and INAA. A third piece ($3\text{--}4 \text{ cm}^2$ in area) was taken from selected fragment samples for thin-section preparation.

Optical microscopy of the shards was used in order to check by optical means if it was possible to distinguish between different sources of materials. Optical microscopy was also used to identify any special characteristics which might be indicative of ceramic production, as was referred to by Velde and Druc (1999). Also, the petrographic microscope allowed selection of microsites to examine by SEM and, consequently, to perform

chemical analyses. Samples for thin-section preparation were consolidated with an epoxy resin (Velde and Druc, 1999) in order to secure the grains in the paste. The SEM-EDS was carried out on polished thin-sections. The SEM images and chemical spectra of graphite-coated specimens were taken using a LEICA Cambridge S360 microscope.

To obtain powder samples of ceramics for XRD and INAA, the procedure is as follows: the inner and outer surfaces of the shard are scraped using a drill burr made of tungsten carbide. The scraped specimens are subsequently brushed clean, washed, boiled for 30 min in deionized water, and then dried for several hours at 30°C . After drying, a planetary agate mortar for small samples was used to crush and homogenize $\sim 2 \text{ g}$ of pottery sample into a fine powder ($<53 \mu\text{m}$). Sub-samples were taken for XRD and INAA.

Potential source clays ($500\text{--}1000 \text{ g}$ depending on the grain size) were dried at 30°C and ground in agate mortars into a fine powder ($<53 \mu\text{m}$). Sub-samples were taken for XRD analyses (whole sample and clay-sized fraction) and INAA. Oriented aggregates of the $<2 \mu\text{m}$

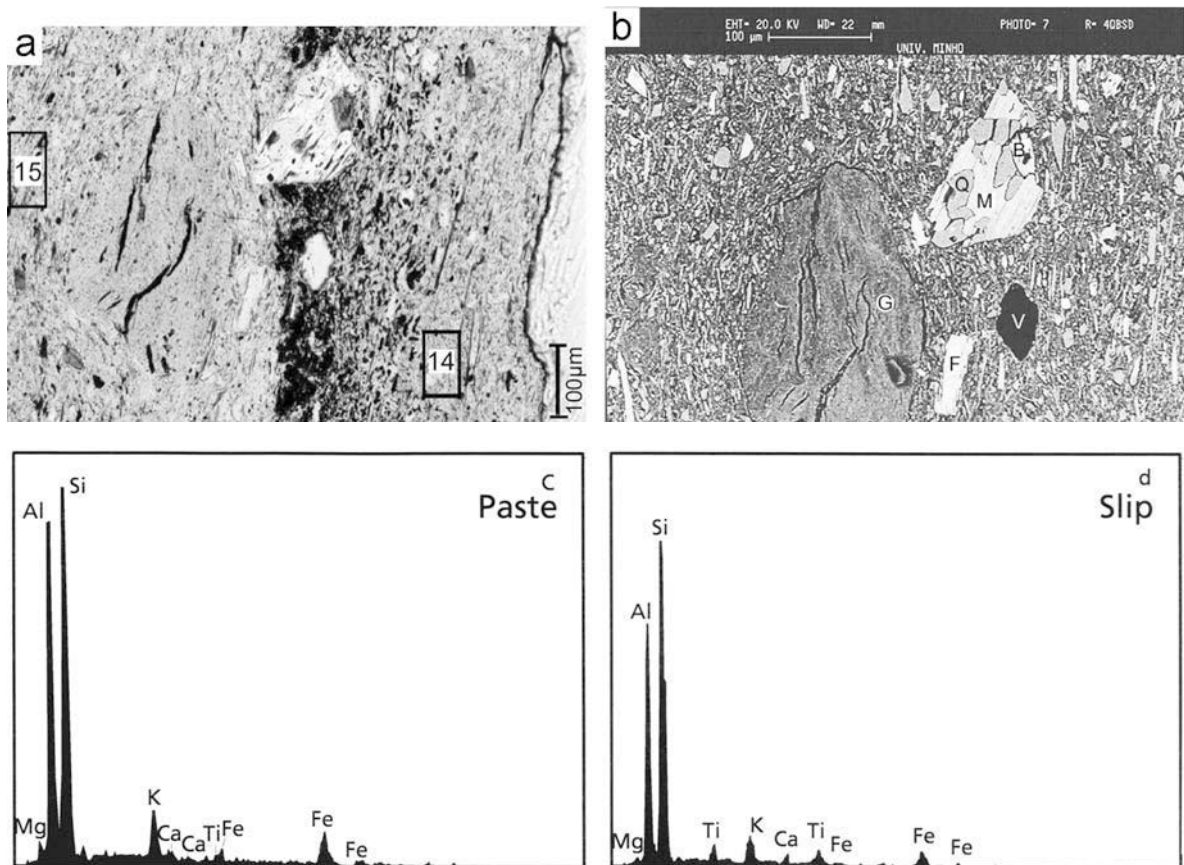


Figure 2. (a) Photomicrograph of polished thin-section, under plane-polarized light, of the sample BB2 showing the paste-slip interface (position 14); (b) BSE image of the same section obtained by SEM-EDS; shrinkage cracks of the clay mass in the grog are well illustrated; (c) X-ray spectrum of the paste: position 15 in (a); (d) X-ray spectrum of the slip: position 14 in (a). M = muscovite; B = biotite; Q = quartz; F = feldspar; G = grog; V = void.

fraction of the raw materials were obtained by sedimentation from an aqueous suspension onto glass slides and subjected to the following treatments: air drying, ethylene glycol solvation and heating (490°C). The XRD patterns were obtained with a Philips PW 1710 (APD-version 3.6j) diffractometer using $\text{CuK}\alpha$ radiation at 40 kV and 30 mA, a step size of $0.02^\circ 2\theta$ and counting time of 1.250 s. Analytical software, 'X'Pert Graphics' and 'Identify' by Philips, were used. To estimate the mineral quantities we classified the amounts of minerals detected into four grades (very abundant, abundant, present, trace) based on the peak height percentage for diagnostic reflections of each mineral, obtained by the relative intensity of those peaks in the XRD patterns. In the whole rock, the diagnostic peaks used were the following: quartz – 4.25 Å, alkali feldspar – 3.24 Å, plagioclase – 3.18–3.20 Å, mica – 10 Å, mullite – 5.38–5.41 Å, spinel – 2.02–2.03 Å, anatase – 3.52 Å and hematite – 2.69–2.70 Å. Because the most important reflection of hematite (2.70 Å) is coincident with one reflection of mullite (2.69 Å), the diagnostic peak used to estimate Fe oxide was 2.518 Å. Estimation of clay minerals was done from the relative intensity of the diagnostic peaks related to their basal reflections in the $<2 \mu\text{m}$ fraction (+++ very abundant (>75%); ++ abundant (25–75%); + present (5–25%); tr = traces (<5%)).

Na, K, Fe, Sc, Cr, Co, Zn, As, Br, Rb, Cs, Ba, La, Ce, Nd, Sm, Eu, Tb, Yb, Lu, Hf, Ta, Th and U abundances were determined by INAA. Relative precision and accuracy were, in general, to within 5%, and occasionally within 10%. For INAA, aliquots of ~1 g of powder of ceramics were then dried in an oven at 110°C for 24 h and stored in a desiccator until the samples could be weighed for irradiation. The same procedure was performed for clays and reference materials. Two reference materials, namely soils GSS-4 and GSS-5 from the Institute of Geophysical and Geochemical Prospecting (IGGE) were used. The reference values were taken from data tabulated by Govindaraju (1994).

All powdered samples (ceramics, clays and standards) were prepared by weighing 200–300 mg of powder into cleaned high-density polyethylene vials. Long irradiations (7 h) on pottery and clay specimens are performed in batches of 20 unknowns along with four standards in the core grid of the Portuguese Research Reactor at a thermal flux of $3.34 \times 10^{12} \text{ M cm}^{-2} \text{ s}^{-1}$; $\phi_{\text{epi}}/\phi_{\text{th}} = 1.4\%$; $\phi_{\text{th}}/\phi_{\text{fast}} = 12.1$. The bundles were rotated continuously during irradiation to ensure that all samples received the same exposure to neutrons. Even so, Fe flux monitors were placed in appropriate plastic containers for irradiation together with the samples for neutron flux variation corrections.

Corrections were made for the spectral interference from uranium fission products in the determination of barium and rare earths (Gouveia *et al.*, 1987; Martinho

et al., 1991). Further details of the analytical method were published elsewhere (Prudêncio *et al.*, 1986, 1988).

Multivariate statistical methods were employed (Statistica program by Statsoft, 2003). Each value in the series is standardized: $x = (x-M)/SD$, where M and SD are the overall mean of each variable and the standard deviation for the untransformed series, respectively. Two clustering methods, using as variables the absolute concentration of the chemical elements, as well as normalized contents relative to the Sc content, were employed. The joining (tree clustering) method was used, the amalgamation being done by the unweighted pair-group average, also referred as UPGMA. In this amalgamation method, the distance between two clusters is calculated as the average distance between all pairs of objects in the two different clusters. The similarity coefficient calculated was the Pearson correlation coefficient to evaluate correlation between samples. The results are represented as dendograms (hierarchical tree plots). k-means clustering analysis was the second clustering method used to produce exactly k different clusters of greatest possible distinction, with the

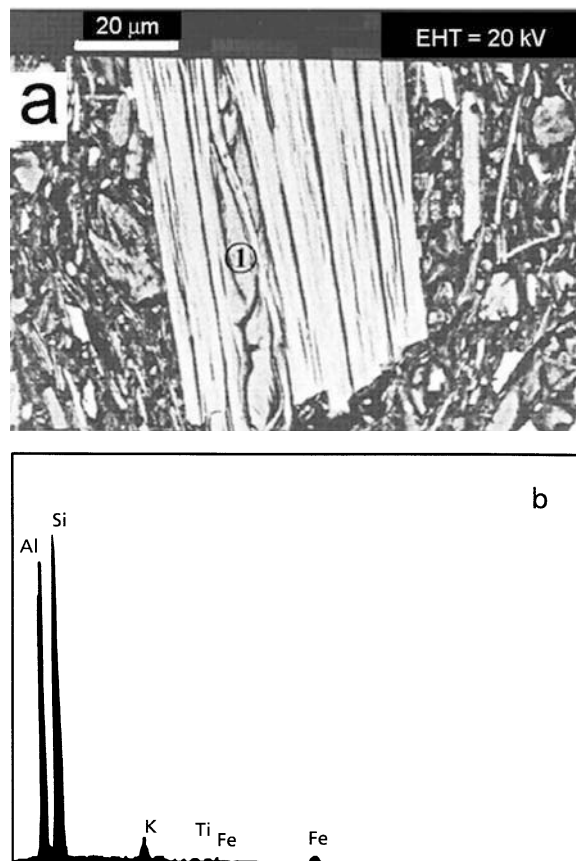


Figure 3. (a) BSE image of a polished thin-section of the Bracaraense ceramic (sample BB2) showing one temper grain of muscovite and material with an Al-Si composition (b) between the cleavage surfaces (position 1).

Table 1. Mineralogical composition of selected Bracaraense pottery shards.

Sample Number	Qz	Fel	Pl	Mic	Mul	Spi	Hem	An
Bracara Augusta								
BB1	+++	+	—	—	tr	—	tr	—
BB2	++	++	—	+	—	tr	tr	—
BB3	++	+	—	—	+	—	—	—
BB4	++	+	—	—	tr	+	tr	—
BB5	++	+	—	—	tr	+	tr	—
BB7	++	+	—	+	tr	tr	—	—
BB8	++	+	—	—	+	+	—	—
BB9	++	++	—	+	+	—	tr	—
BB10	++	+	—	+	—	tr	tr	—
BB12	++	++	—	+	—	+	tr	—
BB13	++	++	—	+	tr	+	tr	—
BB14	++	++	+	+	—	tr	+	—
BB15	++	++	—	—	+	—	—	—
BB18	++	+	—	+	tr	+	—	—
BB19	+++	tr	—	—	+	+	—	—
BB21	++	+	—	—	tr	+	—	—
BB24	++	++	—	tr	+	—	tr	—
BB26	+++	+	—	++	—	tr	tr	—
Aquis Querquennis								
BA1	++	+	tr	+	+	+	+	—
BA2	++	++	+	+	tr	+	tr	—
BA3	++	++	—	—	+	+	—	—
BA4	++	++	—	+	+	+	tr	—
BA5	++	++	—	tr	+	+	+	+
BA6	++	+	—	—	+	+	—	—
BA7	++	+	—	—	+	+	—	—
BA8	++	++	—	—	+	+	—	—

Qz = quartz, Fel = alkali feldspar, Pl = plagioclase, Mic = mica, Mul = mullite, Spi = spinel-like phase, Hem = hematite, An = anatase (+++ very abundant (>75%); ++ abundant (25–75%); + present (5–25%); tr = trace (<5%).

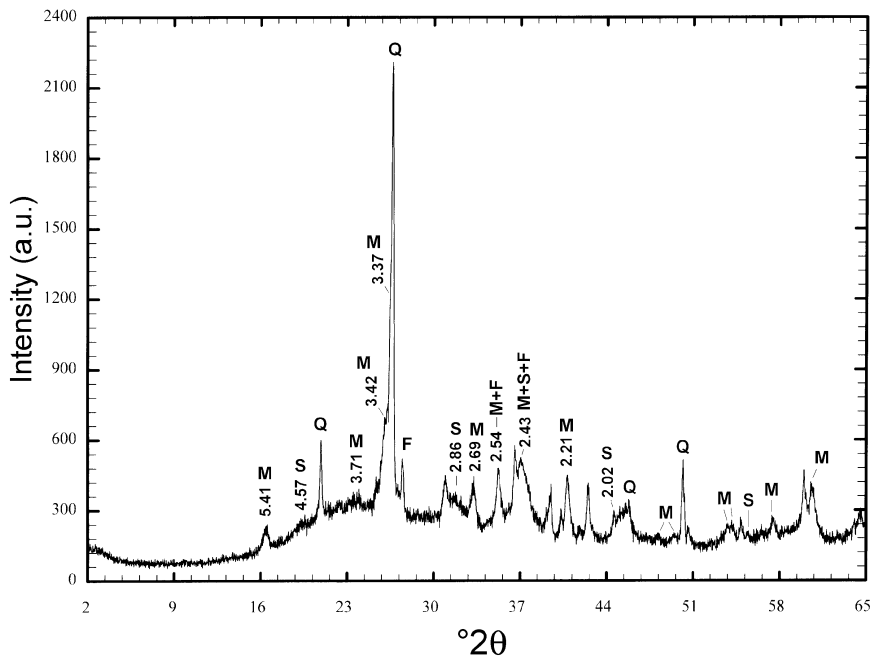


Figure 4. XRD pattern of the Bracaraense ceramic (sample BA6) showing the d values (Å) of quartz (Q), alkali feldspar (F), mullite (M) and spinel (S).

Table 2. Clay mineral abundances derived from oriented samples by XRD.

Geological setting	Location (see Figure 1)	Sample	<2 μm fraction							
			Ill	C-S	V	I-V	Kao	Gib	Goe	
Granite and schist weathering products	Campados	Granites								
		CA1	tr	tr			+++		tr	
		CA2	+	tr			+++		tr	
		CA3	+	tr			+++		tr	
		GB1	+			tr	tr	+++		
		GB2	tr			tr	tr	+++		
	Braga	GB3	tr			tr	+	+++	tr	
		Schists								
	Espinheira	E1	++				++		+	
		E2	+				+++		tr	
		E3	+				+++		+	
		E4	+			tr	++	+	tr	
	Bustelo	B	++				++		tr	
	Sedimentary deposits	Barqueiros	Kaolins							
B1			tr				+++		tr	
B2			tr				+++		tr	
B3			tr				+++			
		B4	+				+++			
Ucha		Kaolinitic clays								
		U1	+				+++		+	
		U2	+				+++		+	
		U3	+		tr		+++		tr	
		Quebrosas	Q1	+				+++		tr
	Q2		+				+++		tr	

Ill = illite; C-S and I-V = randomly interstratified chlorite-smectite and illite-vermiculite; V = vermiculite; Kao = kaolinite; Gib = gibbsite; Goe = goethite (see Table 1 for semi-quantitative mineral composition).

identification of chemical variables most responsible for the discrimination.

RESULTS

Petrography and SEM-EDS

Optical microscopy showed that the Bracaraense ceramics paste is characterized by a very fine- to medium-grained groundmass. The color is generally pale yellow or in some cases yellowish brown. The slip is similar but slightly darker than the paste. The non-plastic grains are quartz (generally with fractures), feldspars (microcline and plagioclase), mica (muscovite and biotite), Fe oxides and grog (fine to medium grain size). Dark spots in the paste matrix were also observed, as well as the presence of voids. The fine grain size character of the paste and the slip, as well as the preferential orientation of the non-plastic grains was confirmed by SEM (Figure 2). Observation by optical microscopy on a polished thin-section also allowed us to characterize the Bracaraense ceramic slip (groundmass boundary in Figure 2a, position 14). It is distinguished from the inner part of the ceramic (paste) by a transition zone with brown hue, sometimes with intersecting non-

plastic grains. This textural difference observed by optical analysis cannot be seen by SEM (Figure 2b). However, SEM-EDS analyses provide the semi-quantitative chemical composition of the paste and slip matrix. The X-ray spectra (Figure 2c–d) show Si-, Al-rich compositions, and small amounts of K and Fe of both paste (area 15 in Figure 2a) and slip (area 14 in Figure 2a). The Al:Si \approx 1 ratio was obtained by EDS on the entire area of the grog (Figure 2b-G). Both compositions may indicate the kaolinitic nature of the clay-rich paste and the slip matrix, as well as of the fired clay or ceramic fragments used as coarser tempering materials (grog).

The BSE image obtained by SEM-EDS (Figure 3) of one Bracaraense shard shows one temper grain of muscovite and a crystalline material with a grain structure among the exfoliated layers of the muscovite. This material is also characterized by an Al-,Si-rich composition (Figure 3b).

X-ray diffraction

Mineral abundance data (estimation of mineral quantities by XRD) for shards from Bracara Augusta and Aquis Querquennis are given in Table 1. There are

no systematic differences in the bulk-sample mineral contents. Quartz and alkali feldspar are present in large amounts in all samples, except one sample in which only traces of alkali feldspar were found; plagioclase only occurs in small amounts in two samples and mica is present in about half of the samples, with a wide range of variation; mullite, spinel and hematite occur in minor quantities in some samples; anatase is present only in one sample. When small quantities of hematite or anatase are present, their reflections cannot be observed by XRD. However, SEM-EDS analysis points to their presence since Fe and Ti phases were found.

A representative XRD powder pattern of the shards is shown in Figure 4. The most distinctive reflections of mullite are: 110, 120, 210, 220, 111, and 121 with d spacings of 5.41, 3.42, 3.37, 2.69, 2.54 and 2.21 Å, respectively. In spite of some quartz and feldspar peaks being coincident with those of mullite, the shape and the relative intensity of their diffraction lines indicate the presence of mullite. The broad peaks suggest poorly crystalline mullite. Spinel can also be inferred from the shape and intensity of the diffraction lines at 4.57, 2.86, 2.43, 2.02 and 1.65 Å. The X-ray data match those of magnesium spinel (MgAl_2O_3 , from PDF 21-1152).

The mineralogical composition of the $<2 \mu\text{m}$ fraction from regional clay materials is given in Table 2. Kaolinite is the most abundant clay mineral, comprising $>75\%$ in the majority of the samples, except in the Braga granite weathering profile, where gibbsite is dominant. Minor amounts of illite are present in all samples, the average percentage present ranging from 5 to 25%. Randomly interstratified chlorite-smectite (C-S) and illite-vermiculite (I-V) were found in trace amounts in some samples of the granite- and schist-weathering products. Traces of goethite were found in 12 of 20 samples studied, while in four samples it ranges from 5 to 25%.

Figure 5 shows the XRD pattern from one randomly oriented specimen of the $<2 \mu\text{m}$ fraction of one sedimentary deposit (Barqueiros kaolins – sample B3, Table 2). The reflections centered at 7.17 and 3.58 Å show the presence of kaolinite. Symmetric and sharp basal reflections and also the well defined 02,11 and 20,13 reflections indicate a high degree of order of this kaolin mineral. The d_{060} reflection at 1.489 Å shows the dioctahedral character of the kaolinite.

These mineralogical features, namely large amounts of highly ordered kaolinite associated with small percentages of impurities (illite and/or goethite), differentiate the sedimentary kaolin deposit from the other raw materials.

Chemical data

Chemical data (averages and standard deviations) obtained in this work for Bracarense ceramic pastes from Bracara Augusta and Aquis Querquennis are given in Table 3. These values can be compared with the same chemical elements contents variations obtained in previous works for the Bracara Augusta common wares (data compiled from Oliveira, 1997; Gomes, 2000; Gaspar, 2000; Oliveira *et al.*, 2005). Despite the small number of pottery shards with Bracarense paste analyzed from Aquis Querquennis, some differences appear to exist compared to those collected in Bracara Augusta, namely higher Fe, Cr, Co, Sc, Ta and Th contents, as well as Br.

The chemical results obtained for the potential source clay materials are given in Table 4. The dendrogram (hierarchical tree plot) shown in Figure 6 clearly shows the clay materials grouped by geological environments: (1) clay materials derived by weathering of schists and sedimentary deposits near Braga; (2) sedimentary kaolins; and (3) clays derived by weathering of the Braga granite and residual kaolins derived by weathering of Campados granite. The means for each cluster of ceramics and clay materials after applying the k-means

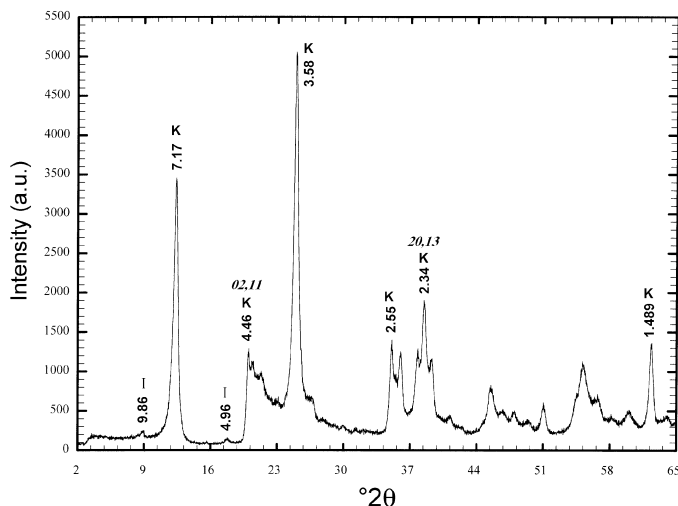


Figure 5. XRD pattern of a random preparation of the $<2 \mu\text{m}$ fraction of the Barqueiros kaolin deposit (sample B3), showing the d values (Å) of kaolinite (K) and illite (I).

Table 3. Average concentration values, *M*, and corresponding standard deviations, σ , of ‘Bracaraense from Bracara Augusta and ‘Bracaraense from Aquis Querquennis’, and ‘Common wares of Bracara Augusta’

	Bracaraense ceramics				Common-wares*				
	Bracara Augusta (27 samples)		Aquis Querquennis (8 samples)		Bracara Augusta (52 samples)				
	<i>M</i>	$\pm \sigma$	<i>M</i>	$\pm \sigma$	<i>M</i>	$\pm \sigma$	<i>M</i>	$\pm \sigma$	
Na ₂ O %	0.20	± 0.039	19	0.15	± 0.02	13	0.36	± 0.178	49
K ₂ O %	2.27	± 0.301	13	2.72	± 0.23	8.4	2.81	± 0.490	17
Fe ₂ O ₃ tot %	3.65	± 0.477	13	5.35	± 0.47	8.7	6.21	± 1.390	22
Sc	15.5	± 1.47	9.5	19.3	± 0.78	4.0	15.9	± 3.14	20
Cr	41.3	± 3.76	9.1	56.5	± 3.12	5.5	52.4	± 14.55	28
Co	7.17	± 1.84	26	10.1	± 2.63	26	9.55	± 2.63	28
Zn	111	± 19.6	18	135	± 22.8	17	121	± 23.54	19
As	16.8	± 5.54	33	11.1	± 3.87	35	19.3	± 9.08	47
Br	3.47	± 2.14	61	18.3	± 7.22	39	5.43	± 2.167	40
Rb	216	± 31.7	15	244	± 26.6	11	224	± 45.8	20
Cs	22.6	± 3.38	15	25.7	± 2.60	10	19.8	± 4.41	22
Ba	341	± 62.0	18	334	± 18.0	5.4	575	± 185.1	32
La	56.7	± 6.41	11	74.7	± 7.20	9.6	77.1	± 15.78	20
Ce	121	± 17.6	15	158	± 23.1	15	149	± 31.2	21
Nd	64.0	± 11.60	18	82.5	± 15.55	19	69.0	± 14.56	21
Sm	14.1	± 3.13	22	17.4	± 3.64	21	12.0	± 2.41	20
Eu	1.95	± 0.497	25	2.27	± 0.45	20	1.63	± 0.333	20
Tb	2.16	± 0.566	26	2.55	± 0.49	19	1.47	± 0.303	21
Yb	6.35	± 1.452	23	7.62	± 1.19	16	4.15	± 0.890	21
Lu	0.85	± 0.166	19	1.00	± 0.15	15	0.62	± 0.144	23
Hf	5.00	± 0.709	14	6.63	± 0.59	8.9	8.67	± 2.857	33
Ta	4.55	± 0.428	9.4	6.33	± 0.23	3.6	3.04	± 0.529	17
Th	33	± 2.9	8.7	43	± 3.9	8.9	35	± 7.3	21
U	15.6	± 2.68	17	18.6	± 2.60	14	9.10	± 1.38	15

* Data compiled from Oliveira (1997); Gomes (2000); Gaspar (2000); Oliveira *et al.* (2005). Concentrations expressed in ppm ($\mu\text{g/g}$) unless otherwise indicated.

clustering method are presented in Figure 7: cluster 1 comprises ceramics and sedimentary kaolins, cluster 2 includes clays derived by weathering of granites, and cluster 3 deposits and weathered schists. The chemical differences between samples are clearly enhanced by this statistical approach, with a particular emphasis on the large *HREE* contents of cluster 1.

In Figure 8 the dendrogram of both the Bracaraense ceramics and clay materials shows that ceramics from both sites are not clearly distinguishable as there are BA and BB samples in both of the major groupings of the Bracaraense materials. Major differences are observed among the groups represented by weathered schists and deposits plus granites when compared to the kaolin and

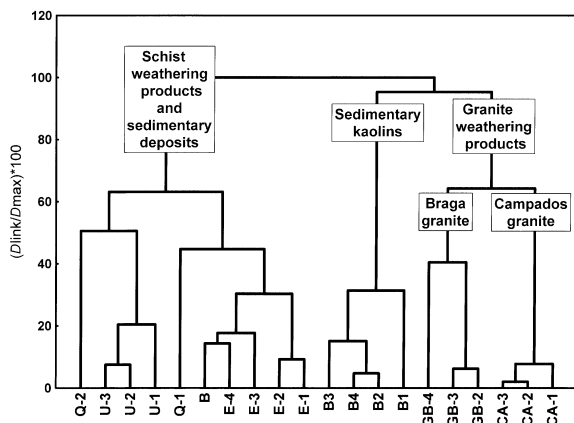


Figure 6. Dendrogram of regional clay materials based on their chemical contents (see Table 4).

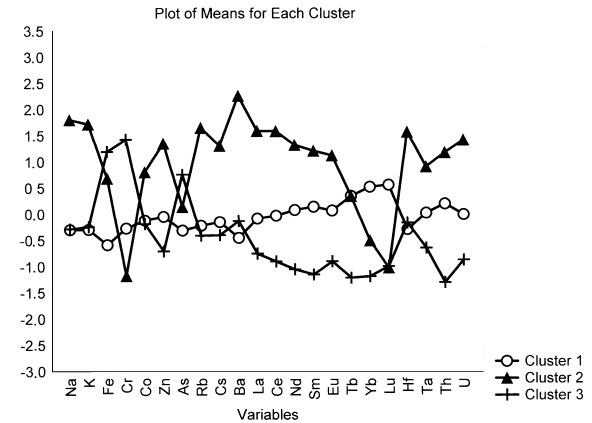


Figure 7. Means for each cluster of ceramics and clay materials after applying the K-means clustering method.

Table 4. Chemical results obtained by INAA for clay materials.

	Granites and schists weathering products										Sedimentary deposits																		
	Campados					Granites					Schists					Kaolins					Kaolinitic clays								
	CA1	CA2	CA3	CA4	CA5	GB1	GB2	GB3	E1	E2	E3	E4	B	Bustelo	B1	B2	B3	B4	U1	U2	U3	U4	U5	Q1	Q2	Q3	Q4	Q5	
Na ₂ O, %	0.34	0.17	0.24	1.34	1.14	0.37	0.29	0.34	0.19	0.13	0.019	0.17	0.12	0.063	0.17	0.12	0.063	0.17	0.18	0.17	0.16	0.17	0.16	0.15	0.13				
K ₂ O, %	6.36	5.31	6.23	4.34	5.5	4.31	3.95	4.41	2.84	2.81	1.54	3.13	2.28	1.19	2.83	2.28	1.19	2.83	2.46	2.46	2.02	2.29	2.02	2.56	1.94				
Fe ₂ O ₃ , %	0.83	0.55	2.12	4.31	4.12	3.09	7	6.99	8.37	11.4	12.3	2.82	1.00	1.10	1.85	5.53	7.08	16.3	5.53	5.53	16.3	7.08	16.3	4.95	7.22				
Sc	2.26	0.55	4.01	10.9	10.4	9.87	11.9	14.8	19.8	25.3	25.7	17.9	14.2	13.8	18.2	14.9	16.9	19	14.9	14.9	16.9	19	13.9	17.7					
Cr	4.22	3.1	5.52	23.7	23.3	20.1	62.3	73.4	76.9	87.9	87.4	53.6	33.6	33.5	50.2	69.5	56.6	55.8	69.5	69.5	56.6	55.8	53.7	77.9					
Co	0.3	0.14	0.22	9.63	8.25	9.42	10.2	10.1	10.2	8.87	14.1	5.16	2.1	4.69	2.91	1.62	3.69	1.94	1.62	1.62	3.69	1.94	8.64	3.52					
Zn	40.6	18.8	40.1	90.8	91.7	70.1	92.1	117	67.4	167	121	182	51.3	63.7	88.9	48.2	56.4	51.7	48.2	48.2	56.4	51.7	103	71.3					
As	3.42	0.01	45.1	7.53	3.49	4.64	11.1	8.29	37.6	30.5	56.8	27.1	2.47	2.65	7.28	88.2	179	368	88.2	88.2	179	368	27.8	21.9					
Rb	407	386	432	295	323	233	166	172	109	112	109	212	149	112	179	80.4	78.7	72.0	80.4	80.4	78.7	72.0	171	97.6					
Cs	45.5	29.8	30.3	13.8	25	13	11.9	11.4	5.86	9.57	6.94	21.6	12.8	11.4	19.9	4.53	4.85	3.75	4.53	4.53	4.85	3.75	20.8	10.7					
Ba	271	169	266	683	791	702	448	516	554	470	329	523	275	240	344	512	485	430	493	512	485	430	493	367					
La	15.5	5.70	12.3	70.2	76.8	90.9	53.7	39.8	31.5	21.5	49.8	111	82.1	76.3	132	39.9	48.8	48.5	39.9	39.9	48.8	48.5	61.6	83.4					
Ce	31.8	13.1	26.4	163	147	174	98.8	78	63.5	54.5	116	243	174	153	252	79.1	95.1	89.1	79.1	79.1	95.1	89.1	113	140					
Nd	15.5	8.00	12.6	72.4	69.4	84.5	43.2	32.2	27.1	17.0	40.9	148	81	57.6	132	39.7	44.9	38.8	39.7	39.7	44.9	38.8	52.4	61.9					
Sm	4.32	2.80	3.69	11.9	11.7	17.8	7.81	6.08	5.72	4.00	8.02	33.2	15.5	14.2	24.9	8.12	8.76	6.94	8.12	8.12	8.76	6.94	9.24	10.1					
Eu	0.64	0.62	0.54	1.33	1.44	2.31	1.54	1.05	0.92	0.73	1.19	5.16	1.65	1.82	2.31	1.47	1.44	1.21	1.47	1.47	1.44	1.21	1.52	1.25					
Tb	0.51	0.40	0.40	0.99	0.94	2.00	0.93	0.86	0.88	0.80	1.10	5.14	1.93	1.65	2.50	0.96	0.87	0.75	0.96	0.96	0.87	0.75	1.16	1.04					
Yb	0.99	0.38	0.77	1.94	2.03	3.79	2.95	3.1	3.5	3.36	3.73	12.7	6.78	4.83	8.38	3.04	2.92	2.48	3.04	3.04	2.92	2.48	3.64	3.33					
Lu	0.071	0.022	0.091	0.25	0.25	0.42	0.47	0.5	0.58	0.54	0.59	1.73	0.94	0.61	1.24	0.46	0.44	0.41	0.46	0.46	0.44	0.41	0.6	0.54					
Hf	2.76	0.75	2.31	8.51	8.82	6.86	7.61	8.17	4.88	4.63	5.11	13.7	13.8	6.03	15.8	7.37	6.14	5.74	7.37	7.37	6.14	5.74	8.14	11.6					
Ta	4.95	1.12	1.98	1.96	2.34	1.66	1.46	1.62	1.42	1.51	1.50	4.98	5.11	4.93	5.5	1.82	1.83	1.85	1.82	1.82	1.83	1.85	2.31	1.96					
Th	6.37	1.24	5.95	41.1	42.8	31.3	15.6	16.7	16.5	15.8	16.2	54.7	54.8	50.7	61.6	15	13.4	13.7	15	15	13.4	13.7	21.6	31.1					
U	5.17	2.55	15.6	15.0	14.9	36.3	4.21	4.78	6.42	6.84	6.00	70.8	11.0	12.3	18.0	4.40	7.45	7.48	4.40	4.40	7.45	7.48	3.76	5.86					

Concentrations expressed in ppm (µg/g) unless otherwise indicated.

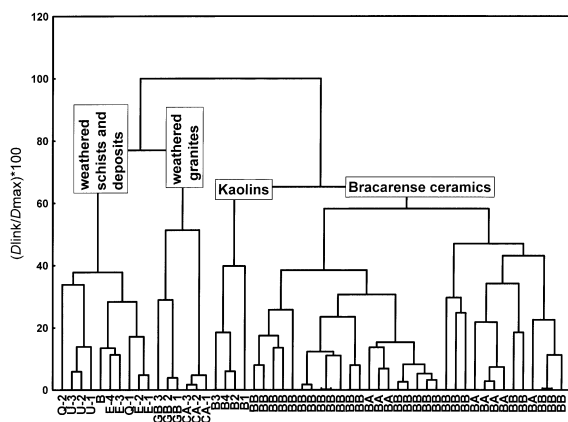


Figure 8. Dendrogram of regional clay materials and Bracarense ceramics (Bracara Augusta – BB; Aquis Querquennis – BA).

Bracarense ceramics. There is a high degree of chemical similarity among the kaolins and Bracarense ceramics, even after normalizing the concentrations of the chemical elements to Sc (conservative element), which diminishes any dilution effect by adding temper.

DISCUSSION

The textural and mineralogical features of the Bracarense ceramics from both archeological sites, Bracara Augusta and Aquis Querquennis, are very similar. The fine-grained character of the paste and slip and the yellow hue are the most common textural characteristics of this type of ceramic paste, pointing to the possible use of the same type of raw material.

The second question addressed in this work is: how does the range of variation in our Bracarense ceramics match with a clay source available in the region? More specifically we looked for raw materials that fall within the range of variation of Bracarense ceramics.

The compositional analyses point to the use of sedimentary kaolins (Barqueiros) for the manufacture of Bracarense ceramics. These clay materials are rich in kaolin minerals, as shown in Figure 5, which reveals a high degree of order in the kaolin minerals. These materials are still used in the ceramics industry. The Al-, Si-rich composition obtained by SEM-EDS (Figure 2) in the paste and slip found in the Bracarense ceramic production, reinforces a kaolin-rich raw material source. Chemical composition also points to the resource of this type of clays as shown in Figures 7 and 8, where the statistical approach using the chemical elements as variables, clearly indicates, with a special emphasis on the role of REE.

Kaolinite was not detected by XRD in ceramics, indicating that they were fired at high temperatures. The temperature at which thermal changes occur for kaolinite is 500–600°C (Brown and Brindley, 1980). Above this temperature the total transformation of these clays

occurs and a new mineral is crystallized. Brown (1980) suggested that mullite ($3\text{Al}_2\text{O}_3 \cdot 2\text{SiO}_2$ to $2\text{Al}_2\text{O}_3 \cdot \text{SiO}_2$) and various cubic spinels or spinel-like phases may be encountered when aluminous clay minerals are heated to 900°C and above. Thus, the Al-, Si-rich material identified in the paste and in muscovite microsites (Figures 2 and 3) is an aluminosilicate, probably mullite, which was identified by XRD. According to Baumgart *et al.* (1984) the mullite composition depends on the amounts of Al and Si, as well as on the temperature raised during firing. It should be noted that the identification of mullite in the archeological ceramics studied was not possible by optical microscopy, as none of its characteristic forms could be found. In addition, only small amounts of mullite were found by XRD (Figure 4). The average percentage of mullite in 19 samples of 26 studied is 6% (Table 1), ranging from 1 to 15%. The same mean value was obtained for spinel.

SEM-EDS analyses have shown the presence of some irregular particles with grain structure and Al-Si composition in the paste. According to Bates (1971) a grain structure can be developed in samples fired up to 800°C, and it becomes more pronounced at higher temperatures. Besides, in some studied Bracarense shards a material with the same grain structure was observed between the muscovite surfaces (Figure 3). The occurrence of kaolin minerals in natural weathering of granites was referred to by Sequeira Braga *et al.* (2002). Those authors showed that the highest percentages of Si and Al correspond to more exfoliated and separated layers of biotite and muscovite. Thus, those materials, with grain structure and Al-,Si-rich composition observed in the temper grains, such as the muscovite (Figure 3), correspond to mullite. In fact, this new mineral results from stages of thermal transformation of the kaolin minerals during firing of the ceramics.

Despite the Al:Si \approx 1 ratio obtained by SEM-EDS in some grains in the paste, together with the absence of kaolinite in the XRD patterns, the chemical composition cannot be directly associated with the crystallization of spinel-like phases, such as $\gamma\text{-Al}_2\text{O}_3$ or Al-Si spinel. The formation of these new minerals as well as of mullite occurs after the dehydroxylation of kaolin minerals (Gomes, 1988). However, the XRD did not allow clear identification of the abovementioned metaphases (spinel-like) associated with mullite of low degree of order in the pottery shards studied. In addition, the XRD patterns match those of Mg spinel (MgAl_2O_4). This mineral forms at 1000°C from illite (Velde and Druc, 1999).

Hematite can also be formed from complete dehydroxylation of illite up to 900°C (Gomes, 1988). According to the mineralogical composition of the sedimentary kaolins (Barqueiros) and the hematite-like diffraction pattern obtained by XRD, the disordered hematite present in the Bracarense ceramics paste probably formed *via* goethite at lower temperatures, instead of *via* illite. The formation of hematite also

occurs when Fe^{2+} in a clay matrix is oxidized by firing in air beginning at 400°C and is completely oxidized at 600°C (Velde and Druc, 1999).

The presence of mullite and spinel-like phases points to firing temperatures of ~900°C and above (Brown, 1980; Sinha and Guha, 1992; Carty and Senapti, 1998). According to Velde and Druc (1999), the mineral crystallization cannot give an absolute indication of maximum temperature of firing, but the reaction series of a given clay mineral. These reactions are influenced by factors like the firing temperature, kiln atmosphere and paste composition. Thus, taking into account the mineral transformation phases present in Bracarense shards, the firing temperature of this type of ceramics paste must have been near 900°C.

The chemical composition of the Bracarense ceramic paste is clearly different from the Bracara Augusta common-ware paste mainly due to a lower *REE* fractionation and a greater intermediate and heavy *REE* relative to the light *REE*. Greater U and Ta, and smaller Fe, Na and Ba contents were also found (see Table 3).

The Aquis Querquennis pottery shards analyzed present the same geochemical pattern as those from Bracara Augusta. The differences found between the ceramics from both sites may be due to lateral or in-depth chemical variations in the same sedimentary kaolin deposit or between different kaolin deposits which occur along the coast. The large Br contents found in Aquis Querquennis may be due to the use-wear and/or to post-depositional processes. Thus, ceramics of the two sites appear to have been manufactured with the same type of clay material.

The pottery shards from Aquis Querquennis have greater Br contents, the concentration of which may have occurred during the use of the pottery as this archaeological site is located in a thermal-water region. Thus, the results obtained suggest that the Br contents can be employed as a fingerprint of pottery use. Another important point is that the sample preparation of the shards for INAA does not appear to mask this fingerprint.

Multivariate statistical analysis of the clays and the Bracarense ceramics by using the chemical elements contents as variables (except Br due to its possible modifications after the ceramic manufacture) showed that the ceramics from both sites are not clearly distinguishable (Figures 7 and 8). Moreover, it clearly shows the different types of clay sources grouped by geological environments and the similarity of the Bracarense shards and the sedimentary kaolins.

Among the clay materials studied, the sedimentary kaolin deposits (Barqueiros) and the residual kaolin deposit derived by weathering of the Campados granite are clearly differentiated from the others by their high clay-fraction contents with kaolin minerals (Sequeira Braga, 1988). The results obtained in this work point to the use of clays of sedimentary kaolin deposits occurring

along the NW Iberian Peninsula coast. Thus, in Roman times these deposits appear to have been exploited for pottery, producing a fine ceramic paste used to obtain different types of pots, including imitations of sigillata, terra sigillata, and thin walls from the Augustus Tiberius period, as well as common wares.

Although no ceramic kilns were found in Braga, given the large number of occurrences of ceramics, as well as the importance of the site, production centers probably did exist in the area. To produce pottery with finer pastes, the procurement of appropriate raw materials may have led to the exploitation of the sedimentary kaolin deposits which occur near the coast of the north of Portugal and Galiza. White fine clays are rare and valuable, not only nowadays, but also in antiquity. This might explain its use in the area, even though the source is not very close (~40 km away) to the Bracara Augusta archeological site, especially considering that the manufacture could have taken place in Bracara Augusta.

CONCLUSIONS

The Bracarense ceramics from Aquis Querquennis and Bracara Augusta archeological sites present the same geochemical and mineralogical features, suggesting use of the same type of kaolin-rich raw material. The differences found between the ceramics from both sites can be explained by compositional variations along the same sedimentary kaolin deposit which is widespread along the NW Iberian Peninsula coast.

The most significant chemical variations found, particularly the *REE* contents, are probably due to differences in the amounts of heavy minerals. Differences in clay processing and/or differences in the pottery use and burial environment may explain the differences found in the chemical composition of both sites. In fact, bromine dissimilarity is certainly due to the use-wear and/or to post-depositional processes. Thus, besides these slight differences, a comparison of Bracarense ceramics from the two sites and regional clay materials reinforces the suggestion that sedimentary kaolins were exploited in their manufacture.

Mullite, spinel and hematite were the newly crystallized minerals in the shards, indicating firing temperatures near 900°C, inferred by the reaction series of the kaolin minerals and associated minerals (illite and goethite) during firing.

Sedimentary kaolin deposits along the coast of the NW Iberian Peninsula appear to have been used to obtain a fine, pale yellow paste producing different types of pottery during Roman times, the so-called 'Bracarense' ceramics. While there is no archeological evidence for workshops (kilns, deposits of raw materials, wasters, *etc.*), further analytical study of a larger number of Bracarense ceramics from archeological sites in the region, as well as of the several kaolin deposits, will give

a better delimitation of the geographical area of clay materials resource.

ACKNOWLEDGMENTS

The authors would like to thank the reviewers Professors R. Ferrell and C. Gomes for comments, suggestions and corrections that improved the manuscript.

REFERENCES

- Alarcão, A.M. and Martins, A.N. (1976) Uma cerâmica aparentada com as 'Paredes Finas' de Mérida. *Conimbriga*, **XV**, Coimbra, 91–109.
- Bates, T.F. (1971) The kaolin minerals. Pp. 109–157 in: *The Electron-Optical Investigation of Clays* (J.A. Gard, editor). Monograph **3**, Mineralogical Society, London.
- Baumgart, W., Dunham, A.C. and Amstutz, G.C. (editors) (1984) *Process Mineralogy of Ceramic Materials*, Ferdinand Enke Publishers, Stuttgart, Germany.
- Brown, G. (1980) Associated Minerals. Pp. 361–410 in: *Crystal Structures of Clay Minerals and their X-ray Identification* (G.W. Brindley and G. Brown, editors). Monograph **5**, Mineralogical Society, London.
- Brown, G. and Brindley, G.W. (1980) X-ray diffraction procedures for clay mineral identification. Pp. 305–360 in: *Crystal Structures of Clay Minerals and their X-ray Identification* (G.W. Brindley and G. Brown, editors). Monograph **5**, Mineralogical Society, London.
- Carty, W.M. and Senapti, U. (1998) Porcelain – raw materials, processing phase evolution, and mechanical behavior. *Journal of the American Ceramic Society*, **81**, 3–20.
- Ferreira, N., Dias, G., Meireles, C. and Sequeira Braga, M.A. (2000) Carta Geológica de Portugal na escala 1/50 000. *Notícia Explicativa da Folha 5-D*, Braga, 2ª edição, IGM, Lisboa, 68 pp.
- Gaspar, A. (2000) Contribuição para o estudo de cerâmicas dos séc. V-VI DC de Braga. M.Sc. thesis, Universidade do Minho, Portugal, 93 pp.
- Gomes, A. (2000) Cerâmicas pintadas da época romana: tecnologia, tipologia e cronologia. M.Sc. thesis, Universidade do Minho, Portugal, 93 pp.
- Gomes, C. (1988) *Argilas. O que são e para que servem*. Fundação Calouste Gulbenkian, Lisboa, 457 pp.
- Gouveia, M.A., Prudêncio, M.I., Freitas, M.C., Martinho, E. and Cabral, J.M.P. (1987) Interference from uranium fission products in the determination of rare earths, zirconium and ruthenium by instrumental neutron activation analysis in rocks and minerals. *Journal of Radioanalytical and Nuclear Chemistry, Articles*, **114**, 309–318.
- Govindaraju, K. (1994) Compilation of working values and sample description for 383 geostandards. *Geostandards Newsletter*, **18**, 1–7.
- Hervés Raigoso, F.M. (1989) Escavacion arqueológica do campamento Romano de 'Aquis Querquennis' (Bande, Ourense). *Arqueoloxía*. Informes 3. Campaña 1989, Xunta de Galicia, pp. 45–49.
- ITGE (1989) Mapa geológico de España. Escala 1:200 000, *Hoja nº 17/27*, Ourense/Verin, Madrid, 284 pp.
- Martinho, E., Gouveia, M.A., Prudêncio, M.I., Reis, M.F. and Cabral, J.M.P. (1991) Factor for correcting the ruthenium interference in instrumental neutron activation analysis of barium in uraniferous samples. *Applied Radiations and Isotopes*, **42**, 1067–1071.
- Martins, M. and Delgado, M. (1989–90a) As necrópoles de Bracara Augusta: os achados arqueológicos. *Cadernos de Arqueologia II*, 6/7, Braga, pp. 41–186.
- Martins, M. and Delgado, M. (1989–90b) História e Arqueologia de uma cidade em devir: Bracara Augusta. *Cadernos de Arqueologia II*, 6/7, Braga, 11–38.
- Martins, M. and Delgado, M. (1995) Bracara Augusta: Uma cidade na periferia do império. *Actas do Colóquio Internacional de Arqueologia 'Los finisterres Atlánticos en la Antigüedad (época preromana y romana)'*. Gijón, pp. 121–128.
- Oliveira, F. (1997) Contribuição para o estudo da cerâmica fina de Braga. A cerâmica 'dita Bracarense'. M.Sc. thesis, Universidade do Minho, Portugal, 93 pp.
- Oliveira, F., Sequeira Braga, M.A., Prudêncio, M.I., Delgado, M. and Gouveia, M.A. (2005) The non vitrifiable red slip ware found in Braga (Northwest Portugal). A mineralogical and chemical understanding. Pp. 80–89 in: *Understanding People through their Pottery* (M.I. Prudêncio, M.I. Dias and J.J. Waerenborgh, editors). EMAC'03. Trabalhos de Arqueologia, Série Monográfica, IPA, Lisboa.
- Prudêncio, M.I., Gouveia, M.A. and Cabral, J.M.P. (1986) Instrumental neutron activation analysis of two French geochemical reference samples – Basalt BR and Biotite Mica-Fe. *Geostandards Newsletter*, **X**, 29–31.
- Prudêncio, M.I., Gouveia, M.A. and Cabral, J.M.P. (1988) Instrumental neutron activation analysis of NBS-97a Flint Clay and NBS-98a Plastic Clay reference samples with a view to their use as standards for archeological studies and clay studies. *Journal of Trace and Microprobe Techniques*, **6**, 103–111.
- Prudêncio, M.I., Cabral, J.M.P. and Tavares, A. (1989) Identification of clay sources used for Conimbriga and Santa Olaia pottery making. *Proceedings of the 1986 Archaeometry Symposium* (Y. Maniatis, editor), 503–514.
- Rice, P.M. (1987) *Pottery Analysis, A Sourcebook*. The University of Chicago Press/Chicago and London, 559 pp.
- Rodriguez Colmenero, A. (1983) El campamento romano de 'Aquis Querquennis'. *Actas del II Seminario de Arqueología del Noroeste*. Ministerio de Cultura, Santiago de Compostela, Madrid.
- Sequeira Braga, M.A. (1988) *Arenas e depósitos associados da bacia de drenagem do rio Cávado (Portugal) – Contribuição para o estudo da arenização*. PhD thesis, Universidade do Minho, Portugal, 325 pp.
- Sequeira Braga, M.A., Paquet, H. and Begonha, A. (2002) Weathering of granites in a temperate climate (NW Portugal): granitic saprolites and arenization. *Catena*, **49**, 41–56.
- Sinha, M.K. and Guha, S.K. (1992) Mineralogical studies on five plastic fire clays – DTA, TG and electron microscopy. *Journal of Thermal Analysis*, **38**, 1405–1413.
- StatSoft, Inc. (2003) *STATISTICA* (data analysis software system), version 6. www.statsoft.com
- Velde, B. and Druc, I.C. (1999) *Archaeological Ceramic Materials. Origin and utilization*. Springer-Verlag, Berlin, Heidelberg, 299 pp.

(Received 1 February 2005; revised 27 March 2006; Ms. 1007; A.E. Ray E. Ferrell, Jr.)